



# HHS Public Access

Author manuscript

*J Chromatogr A*. Author manuscript; available in PMC 2016 November 13.

Published in final edited form as:

*J Chromatogr A*. 2015 November 13; 1420: 119–128. doi:10.1016/j.chroma.2015.09.088.

## Development of an enantioselective assay for simultaneous separation of venlafaxine and *O*-desmethylvenlafaxine by micellar electrokinetic chromatography-tandem mass spectrometry: Application to the analysis of drug-drug interaction

Yijin Liu<sup>†</sup>, Michael Jann<sup>‡</sup>, Chad Vandenberg<sup>+</sup>, Chin B. Eap<sup>†</sup>, and Shahab A. Shamsi<sup>\*†</sup>

<sup>†</sup>Center of Diagnostics and Therapeutics, Georgia State University, Atlanta, GA30303 <sup>‡</sup>Health Science Center, University of North Texas, Fort Worth, TX 76107 <sup>+</sup>Midwestern University, Institute for Healthcare Innovation, Glendale, AZ 85308 <sup>†</sup>Unit of Pharmacogenetics and Clinical Psychopharmacology, Dept. of Psychiatry, Lausanne University, Hospital of Cery, Prilly, Lausanne, Switzerland

### Abstract

To-date, there has been no effective chiral capillary electrophoresis-mass spectrometry (CE-MS) method reported for the simultaneous enantioseparation of the antidepressant drug, venlafaxine (VX) and its structurally-similar major metabolite, *O*-desmethylvenlafaxine (*O*-DVX). This is mainly due to the difficulty of identifying MS compatible chiral selector, which could provide both high enantioselectivity and sensitive MS detection. In this work, poly-sodium *N*-undecenoyl-*L,L*-leucylalaninate (poly-*L,L*-SULA) was employed as a chiral selector after screening several dipeptide polymeric chiral surfactants. Baseline separation of both *O*-DVX and VX enantiomers was achieved in 15 min after optimizing the buffer pH, poly-*L,L*-SULA concentration, nebulizer pressure and separation voltage. Calibration curves in spiked plasma (recoveries higher than 80%) were linear over the concentration range 150–5,000 ng/mL for both VX and *O*-DVX. The limit of detection (LOD) was found to be as low as 30 ng/mL and 21 ng/mL for *O*-DVX and VX, respectively. This method was successfully applied to measure the plasma concentrations of human volunteers receiving VX or *O*-DVX orally when co-administered without and with indinavir therapy. The results suggest that micellar electrokinetic chromatography electrospray ionization-tandem mass spectrometry (MEKC-ESI-MS/MS) is an effective low cost alternative technique for the pharmacokinetics and pharmacodynamics studies of both *O*-DVX and VX enantiomers. The technique has potential to identify drug-drug interaction involving VX and *O*-DVX enantiomers while administering indinavir therapy.

**Publisher's Disclaimer:** This is a PDF file of an unedited manuscript that has been accepted for publication. As a service to our customers we are providing this early version of the manuscript. The manuscript will undergo copyediting, typesetting, and review of the resulting proof before it is published in its final citable form. Please note that during the production process errors may be discovered which could affect the content, and all legal disclaimers that apply to the journal pertain.

## Keywords

Enantioseparation; Venlafaxine/O-desmethylvenlafaxine; poly-*L,L*-SULA; MKEC-ESI-MS/MS

---

## 1. Introduction

Venlafaxine (VX, Fig.1B, left), is a prescription medication, which is famous for its effectiveness as an antidepressant drug and is always administered as a racemic mixture [1, 2]. However, the two enantiomers of VX exhibit different pharmacological activity. The *R*-(-) enantiomer inhibits both the noradrenaline and serotonin synaptic re-uptake, while the *S*-(+) enantiomer inhibits the serotonin one [3, 4]. The *O*-desmethylvenlafaxine (*O*-DVX, Fig. 1B, right), which has been developed and marked as a new anti-depressant drug, is the main metabolite of VX. The *O*-DVX is metabolized by the cytochrome P-450 (CYP) in the liver and presents a pharmacological profile similar to VX [2, 5, 6]. Therefore, it is of great significance to develop a chiral assay, which can be used to determine the enantiomeric concentrations of both VX and *O*-DVX in human plasma. In addition, it can help understand pharmacodynamics and pharmacological contribution of each enantiomer [4,7–8]. VX and *O*-DVX and the disposition of its *R*(-) and *S*(+) enantiomers remains to be fully elucidated with only a few animal and human studies as drug-drug interactions are rarely identified in various disease states affecting drug disposition that involve stereospecificity [9,10].

Currently, the most commonly used separation technique for the determination of VX and *O*-DVX in biological samples is high performance liquid chromatography (HPLC), which is based on either achiral or chiral methods with ultraviolet (UV) [11–13], fluorescence [14–15] and MS detection [16–18]. However, the use of HPLC not only requires expensive chiral columns but also careful maintenance of these columns. In addition, HPLC generates large volume of toxic mobile phases, particularly normal phase HPLC-MS using non-polar and flammable mobile phase (e.g., hexane) require safety protocols. More importantly, when the volume of biological samples is limited, the relatively large injection volume requirement in HPLC makes it inferior to capillary electrophoresis (CE).

The use of CE is preferable in drug monitoring compared to chromatographic methods such as HPLC. This is because CE requires less biological samples, and lower operating cost [19–21], application of CE for chiral drug analysis is expected to expand. However, trace level detectability of VX and *O*-DVX by open tubular CE-UV using chiral selectors (e.g., ionic liquid and/or  $\beta$ -CD) in biological samples are not reported [22]. On the other hand, packed column CEC-UV using vancomycin and teicoplanin chiral stationary phases seems to show good potential for analysis of VX and its metabolites in human plasma [23–25]. The use of 0.75% highly sulfated  $\gamma$ -CD as a chiral selector provided nearly baseline separation of VX in 24 min by electrokinetic chromatography (EKC)-MS [26]. Interestingly, upon increasing the concentration of sulfated  $\gamma$ -CD to only 0.85%, second enantiomer was never eluted (due to infinite run time). In addition, no LOD for VX by EKC-MS was reported [26].

Micellar electrokinetic chromatography (MEKC)-MS using chiral polymeric surfactants (aka. molecular micelles) is one of the newly emerging mode in CE-MS, which exhibits higher efficiency, higher resolution and higher enantioselectivity compared to conventional

HPLC-MS [27, 28]. Especially, covalently stabilized micellar aggregates are not fragmented in the gas phase of ESI-MS [29, 30–31]. In addition, MEKC-MS needs very small amount of exotic polymeric surfactant as chiral selectors, which when added to the background electrolyte (BGE) provides pseudophases, which has wide range of hydrophobicity and wider elution window as well as sensitivity similar to HPLC-MS [31].

Despite all of the aforementioned advantages of MEKC-MS, one of the major challenges of this hyphenated technique is to identify chiral surfactants, which provides both high separation selectivity and MS sensitivity. To address this issue, high molecular mass polymeric chiral surfactants should be screened to overcome the limitation of low molecular weight chiral selectors in CE-MS. In this study, three amino acid based polymeric dipeptide surfactants: [polysodium *N*-undecenoyl-*L,L*-leucyl-alaninate (poly-*L,L*-SULA), polysodium *N*-undecenoyl-*L,L*-leucylvalinate (poly-*L,L*-SULV) and polysodium *N*-undecenoyl-*L,L*-leucyl-leucinate (poly-*L,L*-SULL)] with different dipeptide head groups (Fig. 1A), were first synthesized according to previously reported work [32–33]. Next, the MEKC-ESI-MS/MS method for *O*-DVX and VX was successfully developed by varying the polymeric dipeptide surfactant head groups, buffer pH, surfactant concentration and separation voltage. In addition, simultaneous enantioseparation of *O*-DVX, VX and *N*-DVX was profiled suggesting *N*-DVX does not interfere in the quantitation of *O*-DVX and/or VX. Solid phase extraction (SPE) using a strong cation exchange column was used to isolate the enantiomers of *O*-DVX and VX as well as to quantitate both *O*-DVX and VX in plasma samples in MEKC-ESI-MS/MS.

As mentioned earlier, conversion of VX to *O*-DVX is the major biotransformation pathway in human subjects. A minor metabolic pathway in humans is VX conversion to the *N*-DVX metabolite (1%) [34]. The hepatic enzymes responsible for VX metabolism to *O*-DVX and *N*-DVX are the cytochrome P450 (CYP) 2D6 and 3A4, respectively [35]. The *O*-DVX metabolite shows pharmacologic activity that is comparable to VX in several preclinical assessments while the *N*-DVX metabolite displayed much weaker or negligible activity [36]. Therefore, based upon this information, VX and *O*-DVX plasma concentrations were evaluated for this study. The MEKC-ESI-MS/MS method was validated and applied to the potential drug-drug interactions of *O*-DVX or VX when co-administered with indinavir in human volunteer subjects. The drug-drug interaction study previously reported that VX and *O*-DVX did not influence indinavir disposition [9]. However, the reverse effects of indinavir upon VX and *O*-DVX were not previously evaluated.

## 2. Experimental

### 2.1. Reagents and materials

Racemic mixture of VX, *O*-DVX and *R*-atenolol (used as internal standard (IS), HPLC-grade methanol (MeOH), analytical-grade ammonium acetate (as 7.5 M NH<sub>4</sub>OAc solution), triethylamine (99%, TEA), phosphoric acid (85%, H<sub>3</sub>PO<sub>4</sub>), hydrochloric acid (36%, HCl) were all purchased from Sigma-Aldrich (St. Louis, MO, USA). The *R*-(+) enantiomer of VX was purchased from Santa Cruz Biotechnology (Dallas, Texas, USA). The *S*-(-) enantiomer of *O*-DVX was provided by Professor Chin B. Eap, (Unit of Pharmacogenetics and Clinical Psychopharmacology, Dept. of Psychiatry, Lausanne University Hospital, Hospital of Cery,

Prilly, Lausanne, Switzerland). Ammonium hydroxide and acetic acid were supplied by Fisher Scientific (Springfield, NJ, USA). Dipeptides (*L,L*-leucyl-alaninate, *L,L*-leucylvalinate, *L,L*-leucylleucinate) were purchased from Bachem (Torrance, CA, USA). Triply deionized (DI) water used in this experiment was obtained from Barnstead Nanopure II water system (Barnstead International, Dubuque, IA, USA). Strata-X-C polymeric strong cation cartridges (3cc, 60mg) were obtained from Phenomenex (Torrance, CA, USA). The surfactant monomers (*L,L*-SULA, *L,L*-SULV, *L,L*-SULL) were polymerized under 20 M rad using  $^{60}\text{Co}$   $\gamma$ -radiation by Phoenix Memorial Laboratory (University of Michigan, Ann Arbor, MI). Human subject plasma samples were supplied by Mercer University Southern School of Pharmacy (Atlanta, GA, USA) and stored under  $-80\text{ }^{\circ}\text{C}$  until the day when chiral assay was performed.

## 2.2. CE-MS/MS instrumentation

All MEKC-ESI-MS/MS experiments were carried on an Agilent CE system (Agilent Technologies, Palo Alto, CA, USA) interfaced to an Agilent 6410 series triple quadrupole mass spectrometer (Agilent Technologies, 207 Palo Alto, CA) equipped with an Agilent CE-MS adapter kit (G1603A), and an Agilent CE-ESI-MS sprayer kit (G1607). An Agilent 1100 series isocratic HPLC pump was used to deliver the sheath liquid with a 1 :100 splitter. Nitrogen was used as nebulizing gas and drying gas. The Agilent ChemStation software and Agilent Mass-Hunter Workstation (version B.02.01) were employed for instrumental control and data acquisition as well as for qualitative and quantitative data analysis. A 60 cm long fused silica capillary, used in the experiment, (375  $\mu\text{m}$  O.D., with 50  $\mu\text{m}$  I.D) was obtained from Polymicro Technologies (Phoenix, AZ, USA).

## 2.3. MEKC-MS/MS conditions, preparation of background electrolytes and sheath liquids

All MEKC-MS experiments were performed under the normal polarity CE mode. The standards, blank plasma and patient plasma were injected by applying a pressure of 5 mbar for 100 s. Unless otherwise stated, the following ESI-MS conditions were used: the composition and the flow rate of the sheath liquid were 80/20 MeOH/H<sub>2</sub>O (%v/v) containing 5 mM NH<sub>4</sub>OAc at pH 6.8 and 5  $\mu\text{L}/\text{min}$ , respectively. Capillary voltage, +3000 V. The fragmentor voltage, collision energy and product ion formations for all three analytes were optimized using optimizer software of Agilent LC-MS in flow injection mode with the following details: fragmentor voltage, 113 V for *O*-DVX, 117 V for VX and 137 V for I.S.; collision energy, 17 eV for *O*-DVX and VX, 25 eV for I.S using drying gas flow rate of 8.0 L/min; drying gas temperature, 200 $^{\circ}\text{C}$ ; nebulizer pressure, 3 psi. The ESI-MS/MS detection was performed in the multiple reaction monitoring (MRM) positive ion mode to monitor *O*-DVX ( $m/z$  264.2  $\rightarrow$   $m/z$  58.1), VX ( $m/z$  278.2  $\rightarrow$   $m/z$  58.1) and IS ( $m/z$  267.2  $\rightarrow$   $m/z$  145.2) transitions. The BGEs for simultaneous enantiomeric separations of *O*-DVX and VX were : 20 mM NH<sub>4</sub>OAc, 25 mM TEA were prepared by diluting the 7.5 M NH<sub>4</sub>OAc stock solution and 99% TEA in triply deionized water (DI) water. Next, adjusting to various pH values by acetic acid. The final running MEKC-ESI-MS/MS buffer solutions were prepared by addition various concentrations of dipeptide polymeric surfactant to the BGE solution. The sheath liquids were prepared by mixing aqueous 5 mM NH<sub>4</sub>OAc buffer at pH 6.8 with appropriate volume ratio of MeOH/H<sub>2</sub>O.

#### 2.4. Solid phase extraction (SPE)

The SPE was performed with Strata-X-C polymeric strong cation cartridges (3 cc, 60 mg). The cartridges were first activated with 2 mL of MeOH and then with 2 mL of triply DI water. Aliquots of 250  $\mu$ L patient plasma sample, 2.5  $\mu$ L of IS (1mg/mL) and 250  $\mu$ L of 4 % (v/v) H<sub>3</sub>PO<sub>4</sub> were added to a 1.5 mL microcentrifuge tube. After vortexing for 30 s, the mixed solution was centrifuged at 1000 rpm for 10 min. Thereafter, the supernatant (~ 450  $\mu$ L) was loaded on the pretreated Strata-X-C cartridge. Next, the supernatant was adsorbed into the cartridge, which took about 15 sec, the loaded sample on the cartridge was washed with 2 mL of 0.1 M HCl followed by 2 mL of MeOH. After the two washes, the cartridge was dried under gentle stream of air for 30 s. The analytes were then eluted with 2 mL NH<sub>4</sub>OH/MeOH (5/95 v/v) in a 10 mL glass tube and the solvent was evaporated in a vacuum chamber under a gentle stream of air. Finally, the residue in the tube was reconstituted with 50  $\mu$ L of MeOH/H<sub>2</sub>O (10/90, v/v) before injecting for analysis by MEKC-ESI-MS/MS.

#### 2.5. Preparation of standard solutions

Individual stock solution of racemic *O*-DVX, racemic VX and IS were prepared by dissolving the appropriate amount of each authentic standard in pure MeOH at 1.0 mg/mL. A mixture of *O*-DVX, VX and IS was prepared by taking certain aliquot of each stock solution and diluting to the desired concentration in MeOH/H<sub>2</sub>O (10/90, v/v). The elution order of the VX and *O*-DVX enantiomers was determined by spiking the standard racemic mixture with *R*-(+)-VX and *S*-(-)-*O*-DVX, respectively. For example, a comparison of unspiked racemic mixture of *O*-DVX versus the racemic mixture of *O*-DVX spiked with *S*-(-)-*O*-DVX is shown in Fig. S1.

#### 2.6 Calibration curves

Calibration standards were prepared by spiking a 250  $\mu$ L of blank human plasma with 5  $\mu$ L of standard stock solutions (15, 30, 90, 135, 270, 360, 500  $\mu$ g/mL) of racemic mixture of both *O*-DVX and VX, 2.5  $\mu$ L of IS at 1mg/mL to yield the final concentration of 0.15, 0.3, 0.9, 1.35, 2.7, 3.6 and 5  $\mu$ g/mL of *R*-(+)- and *S*-(-)-*O*-DVX and VX. All spiked calibration standards followed the procedure of SPE as discussed above in section 2.4. Finally, the calibration curves were built by taking the ratio of the peak area of each respective enantiomer to the IS versus the spiked concentrations of enantiomer in the blank plasma.

#### 2.7. Extraction recovery and matrix effect

The extraction efficiency of VX and *O*-DVX enantiomers was determined by analyzing three replicates of plasma samples at three concentration levels of 150, 1350 and 5000 ng/mL for both *R*- and *S*- enantiomers. The extraction recovery was calculated by comparing the peak area ratio of the extracted blank plasma sample versus peak area ratio of the unextracted enantiomers standards [where the peak area ratio is defined as individual enantiomer peak area divided by the peak area of IS (atenolol)]. Non-deuterated IS such as imipramine [24], tramadol [4] and atenolol [37] all have been successfully used for the quantitation of VX and *O*-DVX. The reason that prompted us to choose atenolol as IS was its +1 charge similar to VX or *O*-DVX. Furthermore, atenolol eluted in the beginning of the electropherogram before elution of VX and *O*-DVX decreasing the total analysis time.

To evaluate the matrix effects, the *R/S* mixture of VX and *O*-DVX at three concentration levels containing IS at fixed concentration were added to 0.5 mL blank plasma extract, dried and reconstituted with 100 mL of methanol-water (10:90, v/v). The corresponding peak area ratios (a) were compared with those of the standard solutions containing equivalent amount of the two *R/S* standards solutions of the two compounds and the IS dried directly and reconstituted with the same solvent (b). The ratio (a/b) x 100) % was used to evaluate the matrix effect.

### 3. Results and discussion

#### 3.1. Optimization of MEKC-MS/MS conditions for the simultaneous enantioseparation of *O*-DVX and VX

First, enantioresolution, analysis time and electrospray sensitivity of *O*-DVX and VX were compared using three dipeptide polymeric surfactants. Second, using the optimum surfactant head group, the pH of the running buffer was varied. Finally, the concentration of surfactant, nebulizing gas and voltage enabled the simultaneous baseline enantioseparation of both *O*-DVX and VX with the shortest possible run time.

**3.1.1. Effect of polymeric dipeptide surfactant head groups**—According to the previous studies on enantioseparations, head group of amino acid based polymeric surfactants plays a significant role in both chiral resolution and MS sensitivity [29, 38–39]. Accordingly, three different polymeric dipeptide surfactants (i.e., poly-*L,L*-SULA, poly-*L,L*-SULV and poly-*L,L*-SULL) with same *N*-terminal amino acid but different *C*-terminal amino acid were synthesized and evaluated for enantioseparation of both *O*-DVX and VX.

The effect of polymeric dipeptide surfactant head groups on the chiral resolution (*R<sub>s</sub>*) and migration time of *O*-DVX and VX enantiomeric pairs is shown in Fig. 2. Two major trends are noted. First, the migration time of *O*-DVX and VX increases greatly with an increase in the hydrophobicity of side chain of the amino acid located at the *C*-terminal end of the dipeptide surfactant head group. Second, the chiral *R<sub>s</sub>* of both *O*-DVX and VX decreases in the following order: poly-*L,L*-SULA > poly-*L,L*-SULV > poly-*L,L*-SULL. Therefore, poly-*L,L*-SULA, which was the least hydrophobic surfactant was considered to be the best surfactant among the three with respect to shortest migration time and highest chiral *R<sub>s</sub>* of both VX and *O*-DVX. As expected, higher *S/N* of chiral analytes was observed with poly-*L,L*-SULA and poly-*L,L*-SULV compared to poly-*L,L*-SULL due to longest migration time obtained with the latter polymeric dipeptide surfactant.

**3.1.2. Effect of buffer pH**—The pH of the BGE influence the charge on the analyte and chiral polymeric surfactant as well as the magnitude of the electroosmotic flow (EOF). Based on the previous study in our group [30, 39–40], the enantioseparation of most of the cationic compounds was achieved at pH 8.0 using polymeric amino acid surfactant. In this study, there was essentially no enantioresolution of VX when pH was below 8.0 and above 10.0 (data not shown). Therefore, relatively narrow range of pH was investigated from 8.0 to 9.5 to simultaneously enantioseparate VX and *O*-DVX.



Fig.3 shows overlaid electropherograms of pH ranging from 8.0 to 9.5. The migration time of both *O*-DVX and VX slightly increases with an increase of pH from 8.0 to 9.0. This could be possibly explained by an increase in ionic strength (due to pH adjustment of the buffer with  $\text{NH}_4\text{OH}$ ) resulting in a slower electroosmotic flow. Further increase in pH to 9.5 cause changes in the migration time of both *O*-DVX and VX differently. Note that VX is structurally similar to *O*-DVX to a larger extent. However, as mentioned above the trend of migration time is somewhat different at  $\text{pH} > 9.0$  for *O*-DVX compared to VX. Perhaps, the deprotonation of substituted hydroxyl proton located in the benzene ring of *O*-DVX begins at pH 9.5 (resulting in electrostatic repulsion with the poly-*L,L*-SULA). Therefore, slightly zwitterionic character on *O*-DVX results in significant decrease in migration time for this enantiomeric pair. On the other hand, the enantiomers of VX remain partially positive at the same pH resulting in essentially unchanged migration times. Nevertheless, both *O*-DVX and VX have lower efficiency ( $N_{\text{avg}}$ ) and lower chiral  $R_s$  at pH 9.0 compared to pH 8.5. Despite the fact that both *O*-DVX and VX have higher  $S/N_{\text{avg}}$  at pH 9.0 compared to pH 8.5, the latter pH shows a reasonable trade-off between the chiral  $R_s$  and  $S/N_{\text{avg}}$  while maintaining high efficiency.

Under optimized pH of 8.5, multiple reaction monitoring (MRM) precursor to product ion transition was employed for simultaneous separation and multianalyte detection of *O*-DVX, VX and *N*-DVX (Fig. 4). Perhaps, two small enantiomeric peak appeared around 23–25 min in the EIC of VX (bottom most electropherogram) corresponds to the transition of *N*-DVX suggesting some cross talk between MRMs of VX and *N*-DVX. This on line MEKC-MS result is somewhat surprising as the spray chamber optimization in the off-line flow injection LC/MS mode showed no significant abundance from precursor ion ( $m/z = 263$ ) to product ion ( $m/z = 58$ ) transition. Thus, in contrast to LC-MS single ion reaction monitoring (SIR), MEKC-MS/MS provide high selectivity, and a cross talk of product ions but result in no quantitation error as long as the enantiomeric peaks of VX and its metabolites (*O*-DVX and *N*-DVX) are all electro-phoretically resolved. Furthermore, the method can also be used in SIR mode in MEKC-MS. The effect of percent methanol on simultaneous enantioseparation of *O*-DVX and VX is summarized in a series of electropherograms shown in Fig. S2. Although the migration time of both pairs of enantiomer gets longer but essentially no gain in chiral resolution and selectivity was observed.

**3.1.3. Effect of polymeric dipeptide surfactant concentration**—The concentration of polymeric surfactant plays a significant role in chiral  $R_s$  and  $S/N_{\text{avg}}$  ratio in MEKC-MS/MS. The molecular weight of poly-*L,L*-SULA is over 10,000, which is similar to that of poly-*L,L*-SULV, [41]. Hence no spectral clutter or background ions are seen in MEKC-ESI-MS/MS in positive ion mode. Because the polymeric surfactant has zero critical micelle concentration (CMC), very low surfactant concentration can be used in MEKC-MS. Too low concentration of polymeric surfactant can provide high  $S/N_{\text{avg}}$  ratio in MEKC-ESI-MS/MS but it results in unsatisfactory chiral resolution [29]. Thus, the concentration of poly-*L,L*-SULA in the range of 5–35 mM in the running buffer was studied to determine the optimum poly-*L,L*-SULA concentration for the simultaneous separation and detection of the two enantiomeric pairs. As shown in Fig. 5, there is no chiral and achiral  $R_s$  of *O*-DVX and VX at 5 mM poly-*L,L*-SULA but resolution increases significantly at 15 mM. Further,

increasing the poly-*L,L*-SULA concentration from 15 mM to 35 mM, decreases  $N_{avg}$ , chiral and achiral  $R_s$ , as well as  $S/N_{avg}$  but increases migration time of both enantiomeric pairs. For example, at 35 mM poly-*L,L*-SULA the chiral  $R_s$  of *O*-DVX and VX decreases only slightly but the total analysis time increased significantly from 20 min to 31 min and  $S/N_{avg}$  is deteriorated to almost half compared to 15 mM. Because complete baseline separation of both *O*-DVX and VX enantiomers was achieved in the shortest time with highest efficiency and  $S/N_{avg}$ , 15 mM poly-*L,L*-SULA was considered as the optimum polymer concentration.

**3.1.4. Effect of nebulizing gas pressure**—For open tubular MEKC-ESI-MS, when the separation capillary is inserted to the sheath flow interface (i.e., nebulizer), a suction effect at the outlet end of capillary is generated because of nebulizer pressure, which strongly affects chiral  $R_s$ , migration time and  $S/N_{avg}$  [29,40, 42]. In addition, recent report suggest that suction affect can also be generated at the separation capillary outlet where mixing of three fluids (i.e., sheath liquid flow, background electrolyte flow, and drying gas flow) occurs due to differences in the respective velocity of each one of them [43–44]. Therefore, optimizing nebulizing pressure at small increment ranging from 2 psi to 5 psi was investigated. At 2 psi, no signals were observed due to poor nebulization resulting in low electrospray performance. However, as shown in Fig.6, the  $S/N_{avg}$  decreased significantly perhaps due to drop in efficiency when the nebulizing pressure increased from 3 psi to 5 psi but the  $R_s$  changes were minimal. Our results are consistent with the studies of Rudaz and coworkers [45] who found that at low chiral selector concentration the chiral  $R_s$  is less affected by the nebulizer pressure. Moreover, some arcing was observed at 5 psi than at 4 psi. Thus, the peak shape of VX at 5 psi was much worse. A nebulizer pressure of 3 psi was chosen as the best nebulizing pressure because of higher  $N_{avg}$  and  $S/N_{avg}$ .

**3.1.5. Effect of separation voltage**—It is now well-established that higher separation voltage decreases the migration time but could generate joule heating, resulting in variation in migration time, poor peak shape and low  $R_s$  [45]. Based on our study (data not shown), baseline separation of both *O*-DVX and VX enantiomers were maintained when the voltage was increased from 10 kV to 25 kV. To achieve a compromise between good run time repeatability and short analysis time, the voltage was varied in the range of 10–25 kV. It is clear from Fig. S.3 that the total analysis time was over 40 min at 10 kV but it was within 15 min at 25 kV. Moreover, it is worth mentioning that no peak was observed in 50 min even for the first eluting enantiomer at voltage less than 10 kV. Because the analysis time was almost doubled at 15 kV compared to 25 kV, the latter voltage of 25 kV was considered as the optimum voltage though the % RSD of migration time is slightly higher compared to 15 kV.

## 3.2. Method validation

**3.2.1. Extraction Recovery and Matrix effects**—Liquid-liquid extraction (LLE) is simpler and more convenient than SPE for extracting *O*-DVX and VX in human plasma samples. However, the extraction recoveries of *O*-DVX and VX by LLE using ethyl acetate, diethylether and dichloromethane were much lower compared to SPE [4, 47]. Therefore, in this study, SPE was used to extract *O*-DVX and VX in plasma samples at low (150 ng/mL), medium (1350 ng/mL) and high (5,000 ng/mL) concentrations. As shown in Table 1, the



extraction recoveries were between 99% –110% for *O*-DVX and 82% –113% for VX using Strata-X-C polymeric strong cation exchange cartridge. The matrix effects (defined in section 2.7) for the two chiral analytes were in the range of 80–110%. Therefore, no significant matrix effect for VX and *O*-DVX was observed.

**3.2.2. Linearity, LOQ and LOD**—The MEKC-ESI-MS/MS method was developed and applied to determine the concentration of *R/S* enantiomers of *O*-DVX and VX, respectively in blank human plasma samples. Under the optimum conditions, calibration curves (peak area ratios of each enantiomer to IS versus the concentration of enantiomer in blank human plasma) of *R/S* VX and *O*-DVX were generated by a linear regression. The calibration curves summarized in Table 2 displayed good linearity in the range of 150–5,000 ng/mL for each enantiomer of *O*-DVX and VX with respectable determination coefficient ( $r^2$ ) in the range of 0.991–0.994 (Fig.S4). Concentrations of *O*-DVX and VX in patients, which fall below the calibration curve were determined from the response factors or slope of the calibration curve. One of the reviewer is acknowledge for suggesting that the applicability of the method to the clinical framework of therapeutic drug monitoring (TDM) could be partially compromised when using response factor at the lower therapeutic plasma range. The limit of detection (LOD, VX = 10.5 ng/mL and *O*-DVX = 15 ng/mL and limit of quantitation (LOQ, VX = 31 ng/mL and *O*-DVX= 45 ng/mL) were estimated at *S/N* ratio of 3.3 and 10, respectively.

**3.2.3. Precision and Accuracy**—The data for intra- and inter-day precision (measured as % RSD) for relative migration time and relative peak area for VX and *O*-DVX are compiled in top section of Table 2. The inter-day repeatability at medium concentration level was <10% RSD for relative peak area and 3% RSD for relative migration time. Overall, the intra-day repeatability values at low, medium and high concentration levels (defined in Table 1) were <8% RSD and < 5% RSD of relative peak areas and migration times, respectively. In addition, the relative concentration error reported in supplementary Table S.2 were within 15% of the actual (nominal value). Therefore, the precision (Table 2) and accuracy (Table S1) of the MEKC-MS method confirm to the criteria for the analysis of plasma samples in human subjects according to the US-FDA guidelines [48].

### 3.3. Profiling enantiomeric *O*-DVX and VX concentrations in human subject plasma samples

Quantitation of *R*- and *S*-enantiomers in plasma samples of 12 human subjects expected to contain both the parent drug VX and its metabolite *O*-DVX were achieved by the developed MEKC-MS/MS method. In addition, 12 more plasma samples of human subjects treated with *O*-DVX only were studied to measure the *R*- and *S*- concentrations of *O*-DVX. Both classes of human subjects were treated with and without indinavir therapy to measure the enantiomers concentrations and peak ratios of *O*-DVX and VX and the results are briefly discussed below.

In the group of 12 subjects treated with VX and expected to contain both VX as well as *O*-DVX, sample collected at 1 hr and 4 hrs period without indinavir therapy the mean plasma concentration of *R*- and *S*-*O*-DVX were:  $[93.5 \pm 44.5 \text{ ng/mL}, 80 \pm 36 \text{ ng/mL}]$  for  $N= 6$  at

1hr], [59.5 ± 39.5 ng/mL, 54.5 ± 25 ng/mL for N= 10 at 4 hrs], respectively. The N value represents the number of subjects in which *O*-DVX was detected and quantitated. On the other hand, the *R*- and *S*- concentrations of *O*-DVX for both 1 hr and 4 hrs periods were much higher for the same subjects with indinavir therapy: [235.5 ± 112.5 ng/mL, 241.5 ± 129.5 ng/mL for N= 12 at 1hr], [354 ± 140 ng/mL, 353.5 ± 77.5 ng/mL for N= 12 at 4 hrs], respectively. This suggests that with the concurrent administration of *R/S* VX with indinavir, the *R/S* VX is metabolized faster to *R/S O*-DVX.

The mean plasma concentrations of the *R*- and *S*-enantiomers of VX at 1 hr of the parent drug, in VX treated subject (without indinavir) could only be detected and quantitated in 2 out of 12 subjects: (*R*-VX = 47.5 ng/mL + 3.5 ng/mL and *S*-VX 50 ng/mL + 7 ng/mL, N = 2), whereas the mean plasma concentrations of the same drug was even lower at 4 hrs (*R*-VX = 36 ng/mL + 3.5 ng/mL and *S*-VX 28 ng/mL + 7 ng/mL, N = 7). With indinavir therapy the mean plasma concentrations of *R*- and *S*-VX were: [*R* = 104 ± 61.5 ng/mL, *S* = 130 ± 69 ng/mL for N= 9 at 1hr)], [*R* = 195 ± 103 ng/mL, *S* = 285 ± 167.5 ng/mL for N= 12 at 4 hrs], respectively.

For the group of 12 subjects treated with *O*-DVX only, the following trends of *R*- and *S*-*O*-DVX were observed: (a) without indinavir therapy: [*R* = 82.5 ± 48 ng/mL, *S* = 74.5 ± 33.5 ng/mL for N= 6 at 1hr)], [*R* = 39 ± 24.5 ng/mL, *S* = 49.5 ± 38.5 ng/mL for N= 11 at 4 hrs], (b) with indinavir therapy: [*R* = 419 ± 70.5 ng/mL, *S* = 399 ± 95.5 ng/mL for N= 12 at 1hr)], [*R* = 408.5 ± 104 ng/mL, *S* = 431.5 ± 70 ng/mL for N= 12 at 4 hrs].

Peak height ratio in VX treated subjects, the *S*- to *R*-VX and *S*- to *R*-*O*-DVX ranged from 0.56 to 2.43 and 0.50 to 15.2, respectively (Fig.S5–S6), which is in accordance with the literature [49–53]. In one subject (subject # 21, Fig. S7) dosed with the parent drug VX, the low *S/R* ratio of VX was associated with higher *S/R* ratio of *O*-DVX. Further studies are warranted to correlate MEKC-MS findings of enantioselective metabolite ratio versus genotype/-phenotype (i.e., CYP2D6) genes. Alternatively, chiral MEKC coupled to high resolution MS assay could predict a straightforward approach for determination of drug metabolites in studying poor versus fast metabolizers of *R*- and *S*-VX [54].

A comparison of the ratio of the peak height and  $S/N_{\text{avg}}$  of *S*- and *R*- enantiomers of *O*-DVX in the subject 8 dosed with *O*-DVX without and with indinavir therapy is shown as a series of chromatograms in Fig.7. In the subject without indinavir therapy (chromatograms shown on the left column), the *S/R* ratio of peak height changes from 0.83 at 1 hr to 0.98 at 4 hrs. Although significant decrease in the peak height ratio of *S/R* enantiomers is observed in the subject with indinavir therapy at 4 hrs compared to 1 hr but the peak height ratio of *S/R*-*O*-DVX is not reversed and *S/R* ratio of *O*-DVX remains less than one. Clearly, the *S/N* ratio of *O*-DVX with indinavir therapy is significantly higher compared to without therapy for both 1 hr and 4 hrs sample collection. These results indicate that the increased *R*-(-) and *S*-(+) enantiomers of VX and *O*-DVX are influenced by indinavir by a similar magnitude by either reduced drug metabolism or elimination from the body.

The mechanism for the increased VX and *O*-VDX of *R*-(-) and *S*-(+) plasma concentrations may be from various sources. VX is metabolized to *O*-VDX by CYP2D6 and to other

metabolites *N*-desmethyl VX and *N,O*-didesmethyl VX by CYP3A4 [55]. Although the biotransformation occurs mainly from VX to *O*-DVX, the other two routes contribute to the overall VX disposition [34]. In-vitro studies showed that the potent CYP3A4 inhibitor ketoconazole reduced *N*-desmethyl VX formation by 42% but the effects on *N,O*-didimethyl VX was not reported [35]. VX, *O*-DVX, and its enantiomers were reported to be substrates of the drug transporter P-glycoprotein (Pgp) without stereoselective evidence [56]. In vitro models with indinavir reported that the protease inhibitor to be a potent inhibitor of both CYP3A4 and Pgp [57–58]. Therefore, increased plasma concentrations of VX, *O*-DVX and its enantiomers can take place by either CYP3A4 and or via Pgp inhibition. The plasma VX and *O*-DVX reported in the previous study only investigated the presence of each drug encountered in VX or *O*-DVX therapy [9]. These findings were similar to other studies with VX and *O*-DVX in routine drug therapy monitoring programs [59–60]. The 1 hr and 4 hrs time points for blood sampling of VX and *O*-DVX were selected to determine the estimated amounts of their enantiomers. Several samples for the 1 hr time point had undetectable concentrations of either VX or *O*-DVX (Fig. S5–S7), which is likely explained by the extended-release formulation of both VX and *O*-DVX where the time point was too early to the T<sub>max</sub>.

The representative electrochromatograms of two subjects treated receiving VX plus indinavir at 1hr are shown in Fig. 8. Clearly, in subject 21, the lower *S/R* ratio of VX is associated with a higher *S/R* ratio of *O*-DVX (top electropherogram). Similar trend was observed in the same subject without indinavir therapy at the same time period. On the other hand, in case of subject 8, the *S/R* ratio of VX is higher but the *S/R* ratio of *O*-DVX is not reversed. The different findings from these two subjects (subject 21 vs. 8) could be reflected by their different pharmacogenetic profiles in CYP2D6 metabolism or Pgp polymorphism. It is unfortunate that pharmacogenetic evaluations were not included in this study.

#### 4. Conclusions

For the first time, the simultaneous stereoselective assay of VX and its major metabolites *O*-DVX in human plasma by MEKC-ESI-MS/MS was successfully developed and validated using a polymeric surfactant, poly-*L,L*-SULA, as a pseudostationary phase. This method gave simultaneous baseline enantioseparation of both enantiomeric pairs in less than 15 min. Validation involved determination of linearity, precision, LOD and LOQ. The linearity and precision ( $r^2 = 0.993$  and  $0.995$ ) results indicated that the method was reliable for the quantitative analysis of the enantiomers. The LOD and LOQ of 10.5 ng/mL and 31 ng/mL of VX, whereas 15 ng/mL and 45 ng/mL for *O*-DVX, respectively was estimated, which is superior to MEKC-UV using charged cyclodextrins [4]. In addition, a SPE procedure performed using Strata-X-C polymeric strong cation cartridges provided recovery higher than 80% for both *O*-DVX and VX in blank plasma samples. Although being suitable for the study carried out on human volunteers receiving high doses of VX or *O*-DVX, the applicability of the method to the clinical framework of TDM is somewhat compromised by a partial validation regarding the lower limit of the therapeutic plasma range in patients treated with low drug doses [60]. Nevertheless, the MEKC-MS/MS method proves to be effective for enantiomeric concentration and enantiomeric ratio profiling of VX and *O*-DVX in human subjects.

Both plasma concentrations of *R*(-) and *S*(+) VX and *O*-DVX enantiomers at the 4 hr time point displayed significant increases when indinavir was co-administered. The 4 hr time point begins to approach the T<sub>max</sub> for extended-release VX and *O*-DVX. Indinavir is an inhibitor of CYP3A4 and P<sub>gp</sub> increased all the plasma concentrations in a similar magnitude of effect. Interestingly, quinidine, a CYP2D6 inhibitor, was reported to have different reductions in clearance for the *R*(-) and *S*(+) VX enantiomers [61]. Further studies are needed to fully characterize the potential effects of indinavir on VX and *O*-DVX and their enantiomers as our study was limited to only two sampling time points. However, these results possibly indicate a potential drug-drug interaction between indinavir and these antidepressants.

## Supplementary Material

Refer to Web version on PubMed Central for supplementary material.

## Acknowledgments

This work was supported by NIH (Grant # R01-GM062314). Yijin Liu would like to thank Molecular Basis of Disease MBD program for the support on this work.

## References

1. Andrews JM, Ninan PT, Nemeroff CB. Venlafaxine: A novel antidepressant that has a dual mechanism of action. *Depression*. 1996; 4:48–56. [PubMed: 9160640]
2. Liu W, Wang F, Li H. Simultaneous stereoselective analysis of venlafaxine and *O*-desmethylvenlafaxine enantiomers in human plasma by HPLC-ESI/MS using a vancomycin chiral column. *J. Chromatogr. B*. 2007; 50:183–189.
3. Holliday SM, Benfield P. Venlafaxine: a review of its pharmacology and therapeutic potential in depression. *Drugs*. 1995; 49:280–294. [PubMed: 7729333]
4. Rudaz S, Stella C, Balant-Gorgia AE, Fanali S, Veuthey JL. Simultaneous stereoselective analysis of venlafaxine and *O*-desmethylvenlafaxine enantiomers in clinical samples by capillary electrophoresis using charged cyclodextrins. *J. Pharm. Biomed. Anal.* 2000; 23:107–115. [PubMed: 10898160]
5. Deecher DC, Beyer CE, Johnston G, Bray J, Shah S, Abou-Gharbia M, Andree TH. Desvenlafaxine succinate: A new serotonin and norepinephrine reuptake inhibitor. *J. Pharmacol. Exp. Ther.* 2006; 318:657–665. [PubMed: 16675639]
6. Kingbäck M, Josefsson M, Karlssona L, Ahlnera J, Bengtsson F, Kugelberg FC, Carlsson B. Stereoselective determination of venlafaxine and its three demethylated metabolites in human plasma and whole blood by liquid chromatography with electrospray tandem mass spectrometric detection and solid phase extraction. *J. Pharm. Biomed. Anal.* 2010; 53:583–590. [PubMed: 20435422]
7. Hicks DR, Wolaniuk D, Russell A, Cavanaugh N, Kraml M. A high-performance liquid chromatographic method for the simultaneous determination of venlafaxine and *O*-desmethylvenlafaxine in biological fluids. *Ther. Drug Monit.* 1994; 16:100–107. [PubMed: 8160247]
8. Klamerus KJ, Maloney K, Rudolph RL, Sisenwine SF, Jusko WJ, Chiang ST. Introduction of a composite parameter to the pharmacokinetics of venlafaxine and its active *O*-desmethyl metabolite. *J. Clin. Pharmacol.* 1992; 32:716–724. [PubMed: 1487561]
9. Jann MW, Spratlin V, Momary K, Zhang H, Turner D, Penzak SR, Wright A, VanDenBerg C. Lack of a pharmacokinetic drug-drug interaction with venlafaxine extended-release/indinavir and desvenlafaxine extended-release/indinavir. *Eur. J. Clin. Pharmacol.* 2012; 68:715–721. [PubMed: 22173281]

10. Wikell C, Eap CB, Josefsson M, Apelqvist G, Ahlner J, Baumann P, Bengtsson F. Disposition of venlafaxine enantiomers in rats with hepatic encephalopathy after chronic drug treatment. *Chirality*. 2002; 14:347–350. [PubMed: 11968077]
11. Waschgler R, Moll W, Koenig P, Conca A. Quantification of venlafaxine and O-desmethylvenlafaxine in human serum using HPLC analysis. *Int. J.Clin.Pharm.Th.* 2004; 42:724–728.
12. Samanidou V, Nazyropoulou C, Kovatsi L. A simple HPLC method for the simultaneous determination of venlafaxine and its major metabolite O-desmethylvenlafaxine in human serum. *Bioanalysis*. 2011; 3:1713–1718. [PubMed: 21827270]
13. Mandrioli R, Mercolini L, Cesta R, Fanali S, Amore M, Raggi MA. Analysis of the second generation antidepressant venlafaxine and its main active metabolite O-desmethylvenlafaxine in human plasma by HPLC with spectrofluorimetric detection. *J. Chromatogr. B*. 2007; 856:88–94.
14. Waschgler R, Moll W, Koenig P, Conca A. Quantification of venlafaxine and O-desmethylvenlafaxine in human serum using HPLC analysis. *Int.J.Clin.Pharmacol.Ther.* 2004; 42:724–728. [PubMed: 15624289]
15. Qin XY, Meng J, Li XY, Zhou J, Sun XL, Wen AD. Determination of venlafaxine in human plasma by high-performance liquid chromatography using cloud-point extraction and spectrofluorimetric detection. *J. Chromatogr. B*. 2008; 872:38–42.
16. Zhang W, Xiang B, Wang C. Liquid chromatography-mass spectrometry method for the determination of venlafaxine in human plasma and application to a pharmacokinetic study. *Biomed. Chromatogr.* 2007; 21:266–272. [PubMed: 17230450]
17. Kingback M, Josefsson M, Karlsson L, Ahlner J, Bengtsson F, Kugelberg FC, Carlsson B. Stereoselective determination of venlafaxine and its three demethylated metabolites in human plasma and whole blood by liquid chromatography with electrospray tandem mass spectrometric detection and solid phase extraction. *J. Pharm. Biomed. Anal.* 2010; 53:583–590. [PubMed: 20435422]
18. Eap CB, Lessard E, Baumann P, Brawand-Amey M, Yessine MA, O'Hara G, Turgeon J. Role of CYP2D6 in the stereoselective disposition of venlafaxine in humans. *Pharmacogenetics*. 2003; 13:39–47. [PubMed: 12544511]
19. Cherkaoui S, Rudaz S, Veuthey JL. Non aqueous capillary electrophoresis-mass spectrometry for separation of venlafaxine and its phase I metabolites. *Electrophoresis*. 2001; 22:491–496. [PubMed: 11258760]
20. Vonheeren F, Thormann W. Capillary electrophoresis in clinical and forensic analysis. *Electrophoresis*. 1997; 18:2415–2426. [PubMed: 9456056]
21. Thormann W, Zhang CX, Schmutz A. Capillary electrophoresis for drug analysis in body fluids. *Ther. Drug Monit.* 1996; 18:506–520. [PubMed: 8857576]
22. Zuo L, Meng H, Wu J, Jiang Z, Xu S, Guo X. Combined use of ionic liquid and [3-CD for enantioseparation of 12 pharmaceuticals using CE. *J. Sep. Sci.* 2013; 36:517–523. [PubMed: 23303483]
23. Desiderio C, Aturki Z, Fanali S. Use of Vancomycin silica stationary phase in packed capillary electrochromatography. I. Enantiomeric separation of basic compounds. *Electrophoresis*. 2001; 22:535–543. [PubMed: 11258766]
24. Fanali S, Rudaz S, Veuthey J-L, Desiderio C. Use of vancomycin silica stationary phase in packed capillary electrochromatography. II. Enantiomeric separation of venlafaxine and O-desmethylvenlafaxine in human plasma. *J. Chromatogr. A*. 2001; 919:195–203. [PubMed: 11459304]
25. Catarcini P, Fanali S, Persutti C, D'Acquarica I, Gasparini F. Evaluation of teicoplanin chiral stationary phases of 3.5 and 5  $\mu\text{m}$  inside diameter silica microparticles by polar organic mode capillary electrochromatography. *Electrophoresis*. 2003; 24:3000–3005. [PubMed: 12973803]
26. Rudaz S, Calleri E, Geiser L, Cherkaoui S, Prat JLL. Infinite enantiomeric resolution of basic compounds using highly sulfated cyclodextrin as chiral selector in capillary electrophoresis. *Electrophoresis*. 2003; 24:2633–2641. [PubMed: 12900876]
27. Ozaki H, Terabe S. Online micellar electrokinetic chromatography-mass spectrometry with a high-molecular-mass surfactant. *J. Chromatogr. A*. 1998; 794:317–325.

28. Ishihama Y, Katayama H, Asakawa N. Surfactants usable for electrospray ionization mass spectrometry. *Anal. Biochem.* 2000; 287:45–54. [PubMed: 11078582]
29. Hou J, Zheng J, Shamsi SA. Separation and determination of warfarin enantiomers in human plasma using a novel polymeric surfactant for micellar electrokinetic chromatography-mass spectrometry. *J. Chromatogr. A.* 2007; 1159:208–216. [PubMed: 17499757]
30. Rizvi SAA, Zheng J, Apkarian RP, Dublin SN, Shamsi SA. Polymeric sulfated amino acid surfactants: A class of versatile chiral selectors for micellar electrokinetic chromatography (MEKC) and MEKC-MS. *Anal. Chem.* 2007; 79:879–898. [PubMed: 17263313]
31. Wang X, Hou J, Jann M, Hon YY, Shamsi SA. Development of a chiral micellar electrokinetic chromatography-tandem mass spectrometry assay for simultaneous analysis of warfarin and hydroxywarfarin metabolites: Application to the analysis of patients serum samples. *J. Chromatogr. A.* 2013; 1271:207–216. [PubMed: 23246089]
32. Wang J, Warner IM. Chiral separations using micellar electrokinetic capillary chromatography and a polymerized chiral micelle. *Anal. Chem.* 1994; 66:3773–3776.
33. Shamsi SA, Macossay J, Warner IM. Improved chiral separations using a polymerized dipeptide anionic chiral surfactant in electrokinetic chromatography: Separations of basic, acidic and neutral racemates. *Anal. Chem.* 1997; 69:2980–2987. [PubMed: 9253249]
34. Troy SM, Parker VD, Fruncillo RJ, Chiang ST. The pharmacokinetics of venlafaxine when given in a twice-daily regimen. *J Clin Pharmacol.* 1995; 35:404–409. [PubMed: 7650231]
35. Fogelman S, Schmider J, Venkatakrishnan K, von Moltke LL, Harmatz JS, Shader RI, Greenblatt DJ. *O*- and *N*-demethylation of venlafaxine in vitro by human liver microsomes and by microsomes from cDNA-transfected cells: effect of metabolic inhibitors and SSRI antidepressants. *Neuropsychopharmacol.* 1999; 20:480–490.
36. Muth EA, Haskins JT, Moyer JA, Husbands GE, Nielsen ST, Sigg EB. Antidepressant biochemical profile of the novel bicyclic compound Wy-45,030, an ethyl cyclohexanol derivative. *Biochem Pharmacol.* 1986; 35:4493–4497. [PubMed: 3790168]
37. Dziurkowska E, Wesolowski Marek. Simultaneous quantitation of venlafaxine and its main metabolite *O*-desmethylvenlafaxine, in human saliva by HPLC. *J. Sep. Sci.* 2013; 36:1726–1733. [PubMed: 23495235]
38. Jun H, Shamsi SA. Multivariate approach for the enantioselective analysis in micellar electrokinetic chromatography-mass spectrometry. *J. Chromatogr. A.* 2009; 1216:845–856. [PubMed: 19110258]
39. Hou J, Zheng J, Rizvi SAA, Shamsi SA. Application of polymeric surfactants in micellar electrokinetic chromatography electrospray ionization mass spectrometry of benzodiazepines and benzoxazocine chiral drugs. *Electrophoresis.* 2006; 27:1263–1275. [PubMed: 16523462]
40. Akbay C, Rizvi SAA, Shamsi SA. Simultaneous enantioseparation and tandem UV-MS detection of eight  $\beta$ -blockers in micellar electrokinetic chromatography using a chiral molecular micelle. *Anal. Chem.* 2005; 77:1672–1683. [PubMed: 15762571]
41. Shamsi SA, Valle BC, Billiot F, Warner IM. Polysodium *N*-undecanoyl-*L*-leucylvalinate: A versatile chiral selector for micellar electrokinetic chromatography. *Anal. Chem.* 2003; 75:379–387. [PubMed: 12585461]
42. Shamsi SA. Micellar electrokinetic chromatography-mass spectrometry using a polymerized chiral surfactant. *Anal. Chem.* 2001; 73:5103–5108. [PubMed: 11721906]
43. Mokaddem M, Gareil P, Belgaied J-E, Varenne A. A new insight into suction and dilution effects in capillary electrophoresis coupled to mass spectrometry via an electrospray ionization interface. Part I. Suction effect. *Electrophoresis.* 2008; 29:1957–1964. [PubMed: 18425757]
44. Mokaddem M, Gareil P, Belgaied J-E, Varenne A. New insight into suction and dilution effects in CE coupled to MS via an ESI interface. II. Dilution effect. *Electrophoresis.* 2009; 30:1692–1697. [PubMed: 19360773]
45. Rudaz S, Cherkaoui S, Gauvrit J-Y, Lanteri P, Veuthey J-L. Experimental designs to investigate capillary electrophoresis-electrospray ionization-mass spectrometry enantioseparation with the partial-filling technique. *Electrophoresis.* 2001; 22:3316–3326. [PubMed: 11589296]



46. Jun H, Shamsi SA. Multivariate approach for the enantioselective analysis in MEKC-MS: II. optimization of 1, 1'-binaphthyl-2, 2'-diamine in positive ion mode. *J. Sep. Sci.* 2009; 32:1916–1926. [PubMed: 19479771]
47. Liu W, Cai HL, Li HD. High performance liquid chromatography-electrospray ionization mass spectrometry (HPLC-MS/ESI) method for simultaneous determination of venlafaxine and its three metabolites in human plasma. *J. Chromatogr. B.* 2007; 850:405–411.
48. USFDA. <http://www.fda.gov/downloads/Drugs/GuidanceComplianceRegulatoryInformation/Guidances/ucm070107.pdf>
49. Kingback M, Karlsson L, Zackrisson AL, Carlsson B, Josefsson M, Bengtsson F, Ahlner J, Kugelberg AC. Influence of CYP2D6 genotype on the disposition of the enantiomers of venlafaxine and its major metabolites in postmortem femoral blood. *Forensic Sci.Int.* 2012; 214:124–134. [PubMed: 21840145]
50. Kim RB, Fromm MF, Wandel C, Leake B, Wood AJJ, Roden DM, Wilkinson GR. The drug transporter P-glycoprotein limits oral absorption and brain entry of HIV-1 protease inhibitors. *J Clin. Invest.* 1998; 101:289–294. [PubMed: 9435299]
51. Hochman JH, Chiba M, Yamazaki M, Lin JH. Influence of P-glycoprotein on the transport and metabolism on indinavir in caco-2 cells expressing cytochrome P-450 3A4. *J. Pharmacol. Exp. Ther.* 2000; 292:292–318.
52. Von Moltke LL, Duan SX, Greenblatt DJ, Fogelman SM, Schmitter J, Harmatz JS, Shader RI. Venlafaxine and metabolites are very weak inhibitors of human cytochrome P450-3A isoforms. *Biol Psychiatry.* 1997; 41:377–380. [PubMed: 9024962]
53. <http://www.drugbank.ca/drugs/DB00285>
54. Dahmane E, Boccard J, Csajka C, Rudaz S, Decosterd L, Genin E, Duret B, Bromirski M, Zaman K, Testa B, Rochat B. Quantitative monitoring of tamoxifen in human plasma extended to 40 metabolites using liquid-chromatography high resolution mass spectrometry: new investigation capabilities for clinical pharmacology. *Anal. Bioanal. Chem.* 2014; 406:2627–2640. [PubMed: 24633563]
55. Preskorn S, Patroneva A, Silman H, Jiang HQ, Isler JA, Burczynski ME, Ahmed S, Paul J, Nichols AI. Comparison of the pharmacokinetics of venlafaxine extended-release and desvenlafaxine in extensive and poor metabolizers of cytochrome P4502D6 metabolizers. *J. Clin Psychopharmacol.* 2009; 29:39–43. [PubMed: 19142106]
56. Karlsson L, Schmitt U, Josefsson M, Carlsson B, Johan A, Finn B. Blood-brain barrier penetration of the enantiomers of venlafaxine and its metabolites in mice lacking P-glycoprotein. *Eur Neuropsychopharmacol.* 2010; 20:632–640. [PubMed: 20466523]
57. Chiba M, Hensleigh M, Nishime JA, Balani SK, Lin JH. Role of cytochrome P450 3A4 in human metabolism of MK-639, a potent human immunodeficiency virus protease inhibitor. *Drug Metab Dispos.* 1996; 24:307–314. [PubMed: 8820421]
58. Profit L, Eagling VA, Back DJ. Modulation of P-glycoprotein function in human lymphocytes and Caco-2 cell monolayers by HIV-1 protease inhibitors. *AIDS.* 1999; 13:1623–1627. [PubMed: 10509562]
59. Reis M, Lundmark J, Bjork H, Bengtsson F. Therapeutic drug monitoring of racemic venlafaxine and its main metabolites in an everyday clinical setting. *Ther Drug Monitor.* 2002; 24:545–553.
60. Hiemke C, Baumann P, Bergemann NN, Conca A, Dietmaier O, Egberts O, Fric M, Gerlach M, Greiner C, Gründer G, Haen E, Havemann-Reinecke U, Jaquenoud Sirot E, Kirchherr H, Laux G, Lutz UC, Messer T, Müller MJ, Pfuhlmann B, Rambeck B, Riederer P, Schoppek B, Stingl J, Uhr M, Ulrich S, Waschler R, Zernig G. The AGNP-TDM expert group consensus guidelines: therapeutic drug monitoring in psychiatry. *Pharmacopsychiatry.* 2004; 37:243–265. [PubMed: 15551191]
61. Eap CB, Lessard E, Baumann P, Brawand-Amey M, Yessine MA, O'Hara G, Turgeon. . *J. Pharmacogenetics.* 2003; 13:39–47.

### Highlights

Develop first MEKC-MS assay for simultaneous profiling of VX, *N*-DVX and *O*-DVX enantiomers

MEKC-MS conditions was optimized for simultaneous enantioseparation of VX and *O*-DVX

LOD of VX and *O*-DVX are as low as 21 ng/mL and 30 ng/mL, respectively

MEKC-MS quantitated VX and *O*-DVX, and identified interactions during indinavir therapy

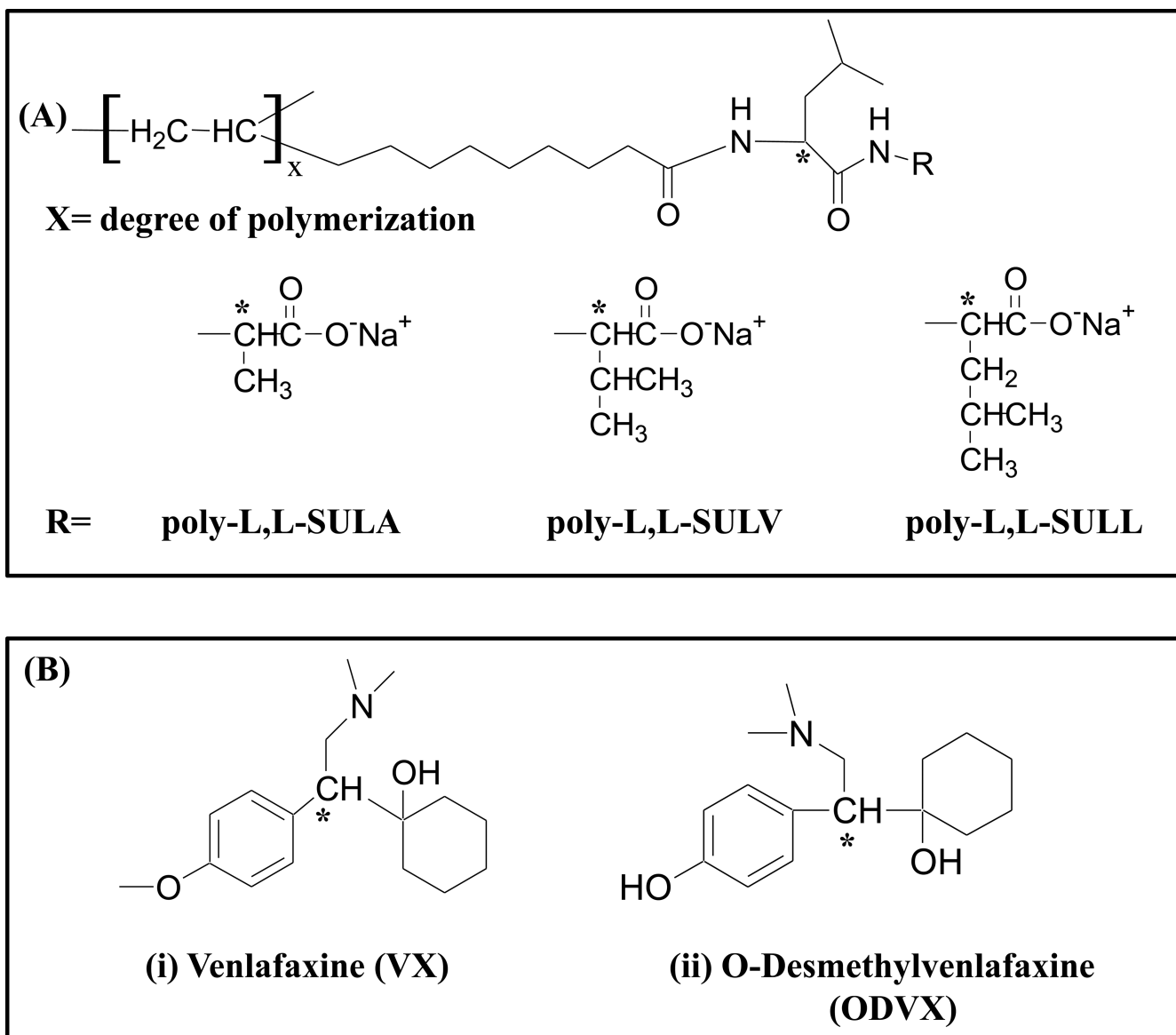


**Fig. 1.** Structure of (A) polymeric dipeptide surfactants with various head groups [poly-*L,L*-SULA, poly-*L,L*-SULV, poly-*L,L*-SULL], and (B) : structures of chiral analytes [venlafaxine (VX) and *O*-desmethylvenlafaxine, (*O*-DVX)].

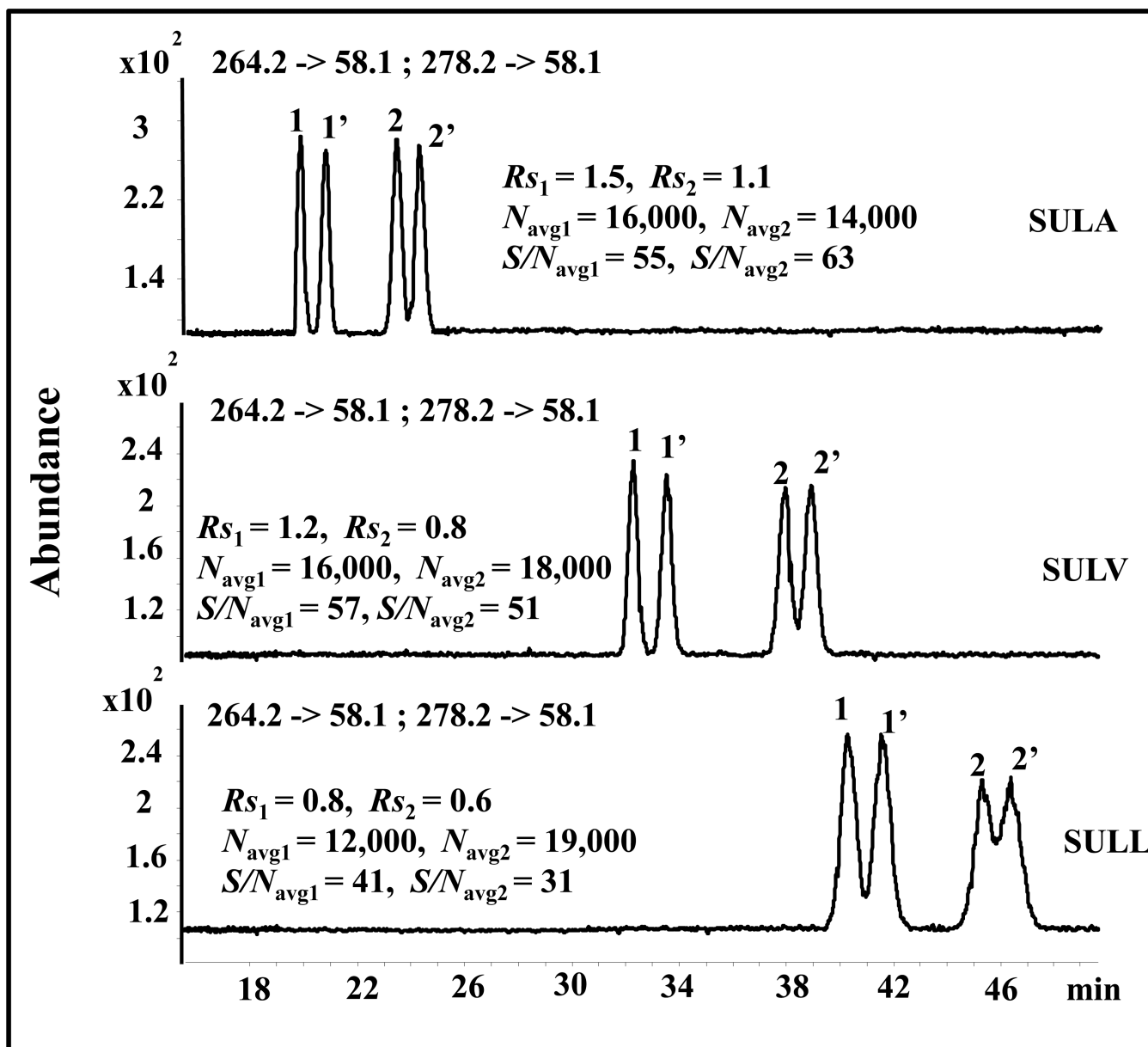


**Fig. 2.** Effect of polymeric dipeptide surfactant head groups on the simultaneous enantioseparation of 1,1' = O-DVX and 2,2' = VX. Conditions: 60 cm long (375  $\mu$ m O.D., 50  $\mu$ m I.D.) fused silica capillary. Buffer: 20 mM NH<sub>4</sub>OAc + 25 mM TEA, pH 8.5, 25 mM poly dipeptide surfactant. Applied voltage, +20 k V, injection, 5 mbar, 100 s. Spray chamber parameters: nebulizer pressure: 3 psi, drying gas temp.: 200 °C, drying gas flow: 8 L/min; capillary voltage: +3000 V; fragmentor voltage, 113 V for O-DVX and 117 V for VX; collision energy: 17 eV; MRM transition: O-DVX: 264.2 -> 58.1; VX: 278.2 -> 58.1. Sheath liquid: MeOH/H<sub>2</sub>O (80/20, v/v), 5 mM NH<sub>4</sub>OAc, pH 6.8 with flow rate of 0.5 mL/min; Sample concentration: 5  $\mu$ g/mL in MeOH/H<sub>2</sub>O (10/90, v/v).

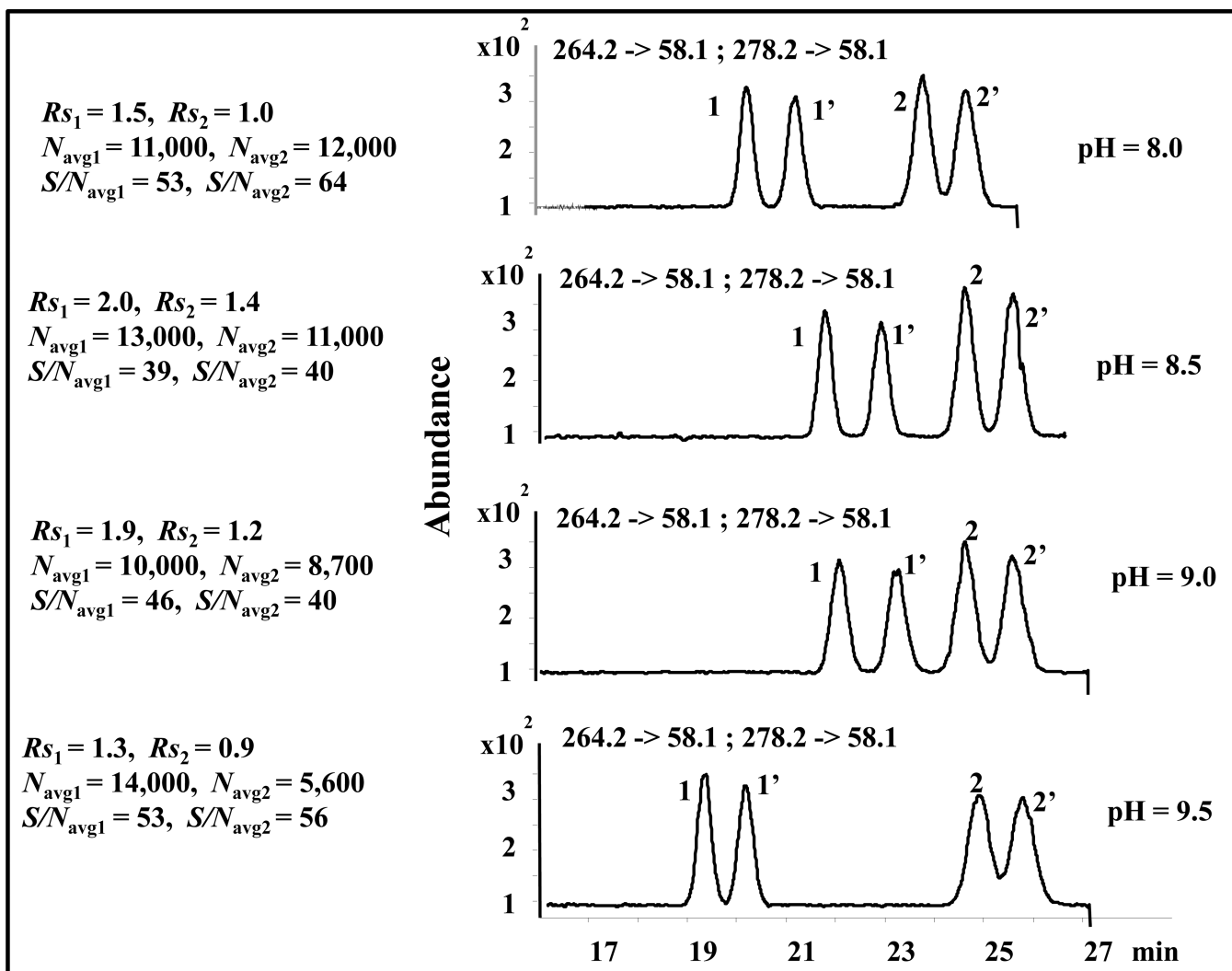


**Fig. 3.** Effect of pH on the simultaneous enantioseparation of 1,1' = ODVX, and 2,2' = VX. The conditions are the same as in Fig. 2 except that 25 mM poly-*L,L*-SULA and different pH ranging from 8.0 to 9.5 were used.

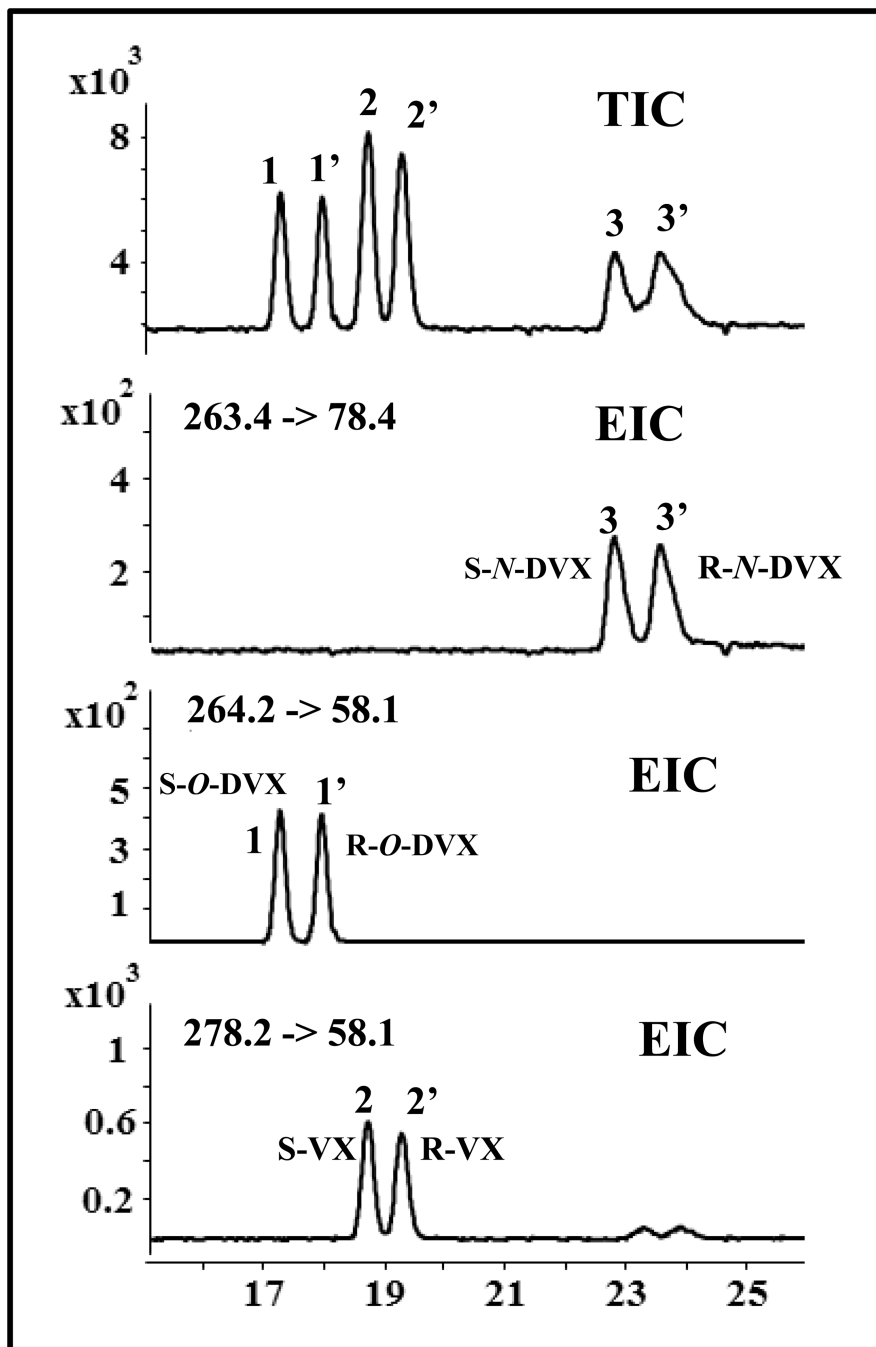


**Fig. 4.** Representative TIC and MRM electropherogram for simultaneous enantioseparation of 1,1' = *O*-DVX and 2,2' = VX and 3,3' = *N*-DVX (*N*-desmethyl-venlafaxine). The MEKC-MS/MS conditions are the same as in Fig. 2 except that 25 mM poly-*L,L*-SULA and 25 kV was used. Fragmentor voltage and collision energy for *N*-DVX: 38 V, and 50 eV, respectively. The MRM precursor to product ion transition for *N*-DVX is 263.4 → 78.4.



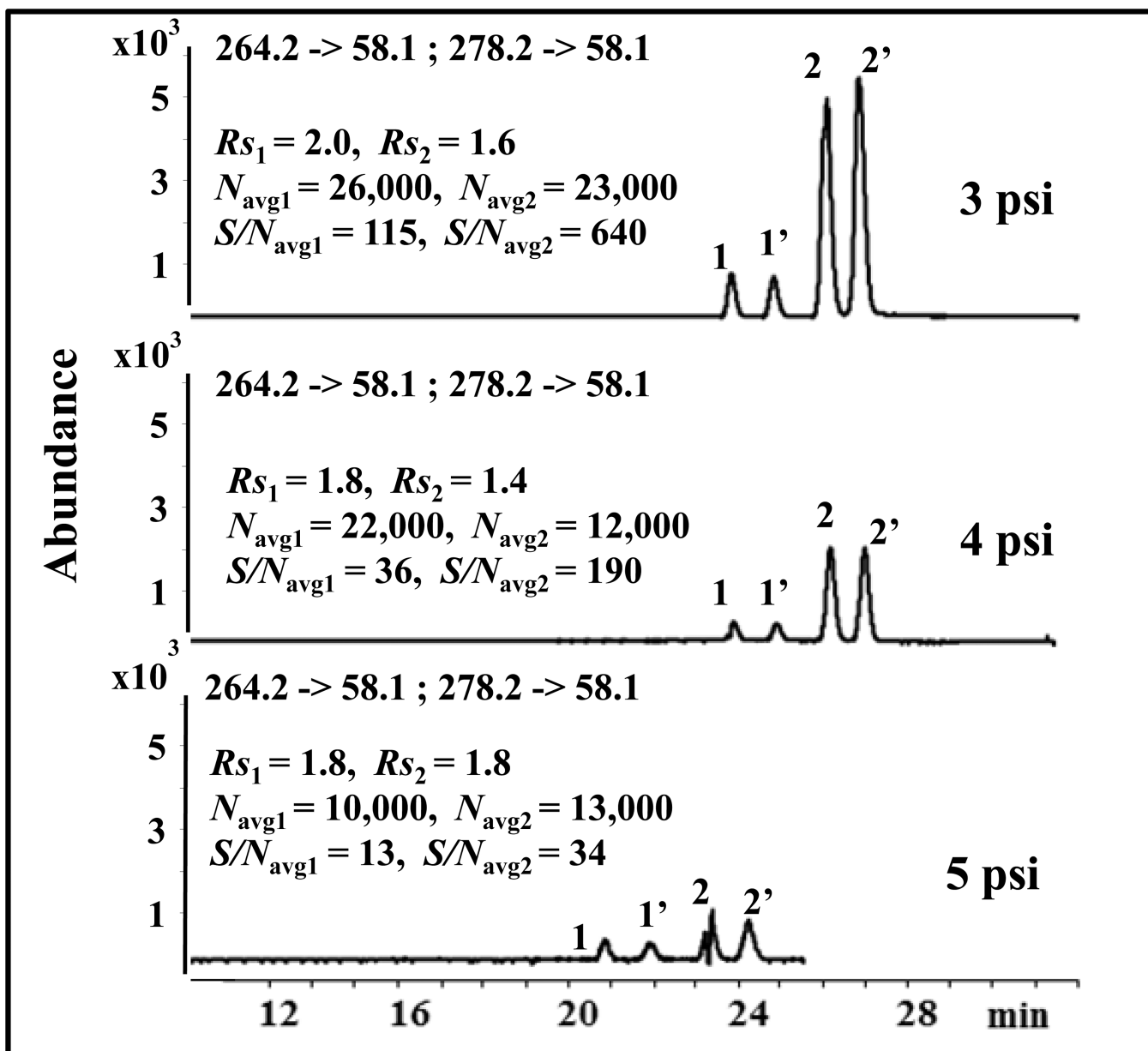


**Fig. 5.** Effect of the concentration of poly-*L,L*-SULA on the simultaneous enantioseparation of 1,1' = *O*-DVX and 2,2' = VX. The conditions are the same as in Fig. 2 except that different concentration of poly-*L,L*-SULA ranging from 5 mM to 35 mM were used.

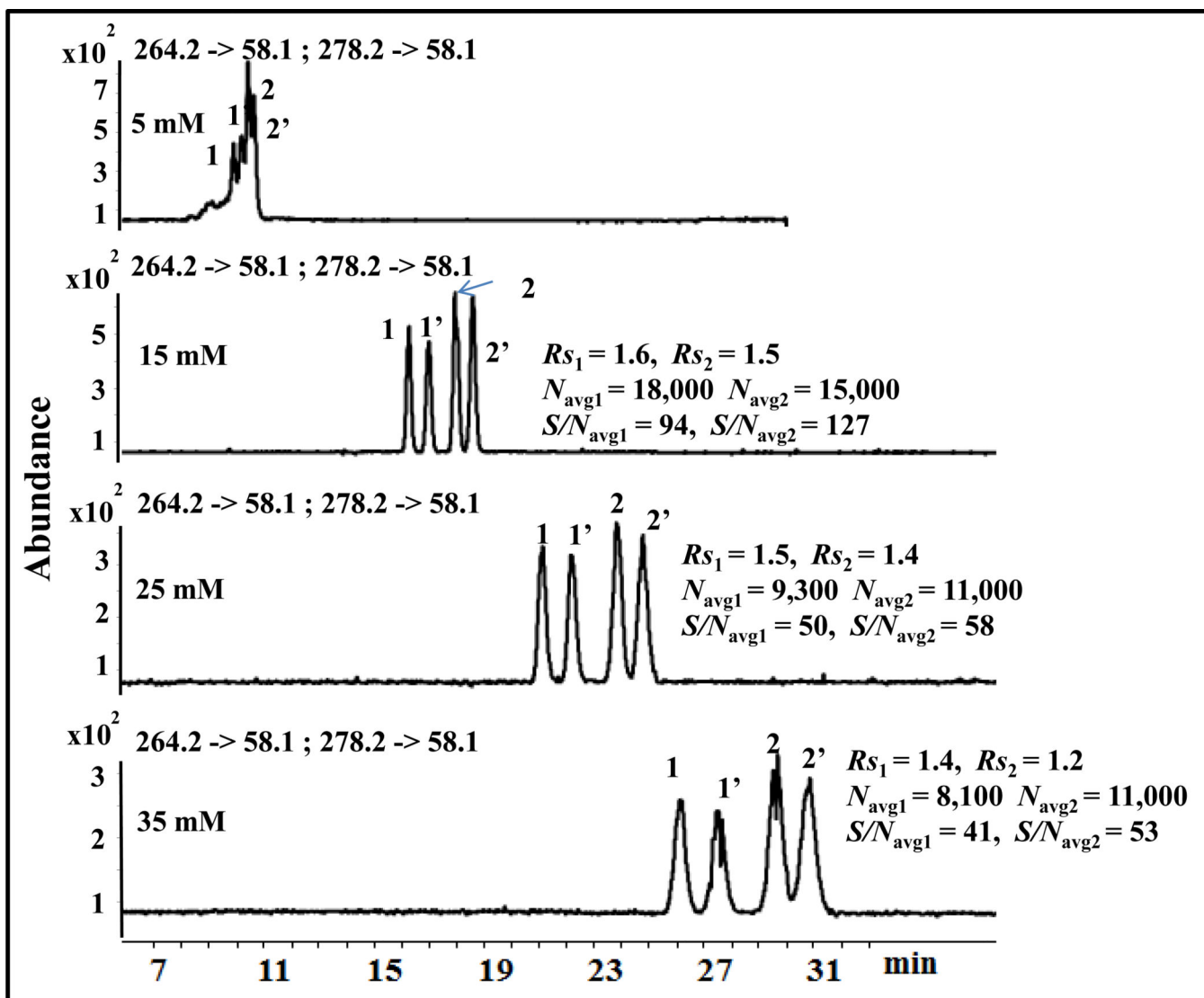


**Fig. 6.** Effect of nebulizer pressure on the simultaneous enantioseparation of 1,1' = *O*-DVX and 2,2' = VX. The conditions are the same as in Fig. 2 except that 25 mM poly-*L,L*-SULA and different nebulizer pressure ranging from 3 psi to 5 psi were used.

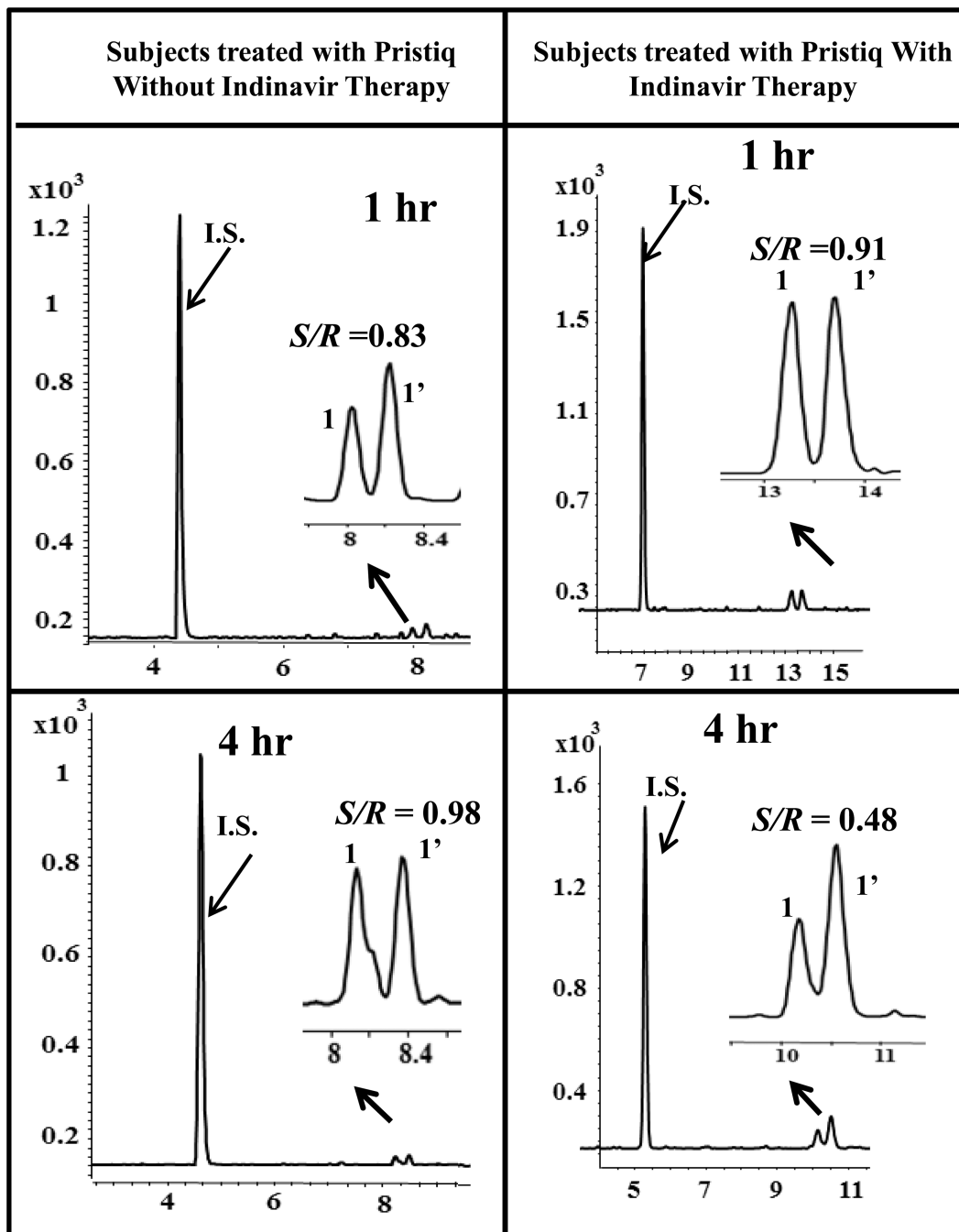


**Fig. 7.**

Total ion electrochromatograms of subject treated with *O*-DVX without and with indinavir therapy at 1 hr and 4 hrs, respectively. The MEKC-MS/MS conditions are the same as in Fig. 2 except that 15 mM poly-*L,L*-SULA and 25 kV was used. The MRM precursor to product ion transition for *R*-atenolol is 267.2  $\rightarrow$  145.2. The enantiomer *S*-*O*-DVX eluted first followed by the *R*-*O*-DVX. (1,1' = *O*-DVX). Without indinavir therapy:  $S/N_I = 118$ ,  $S/N_{I'} = 171$  at 1hr and  $S/N_I = 199$ ,  $S/N_{I'} = 210$  at 4 hr. With indinavir therapy:  $S/N_I = 207$ ,

$S/N_{I'} = 210$  at 1hr and  $S/N_I = 367$ ,  $S/N_{I'} = 630$  at 4 hr for *S*- and *R*- enantiomer of *O*-DVX, respectively

Author Manuscript

Author Manuscript

Author Manuscript

Author Manuscript

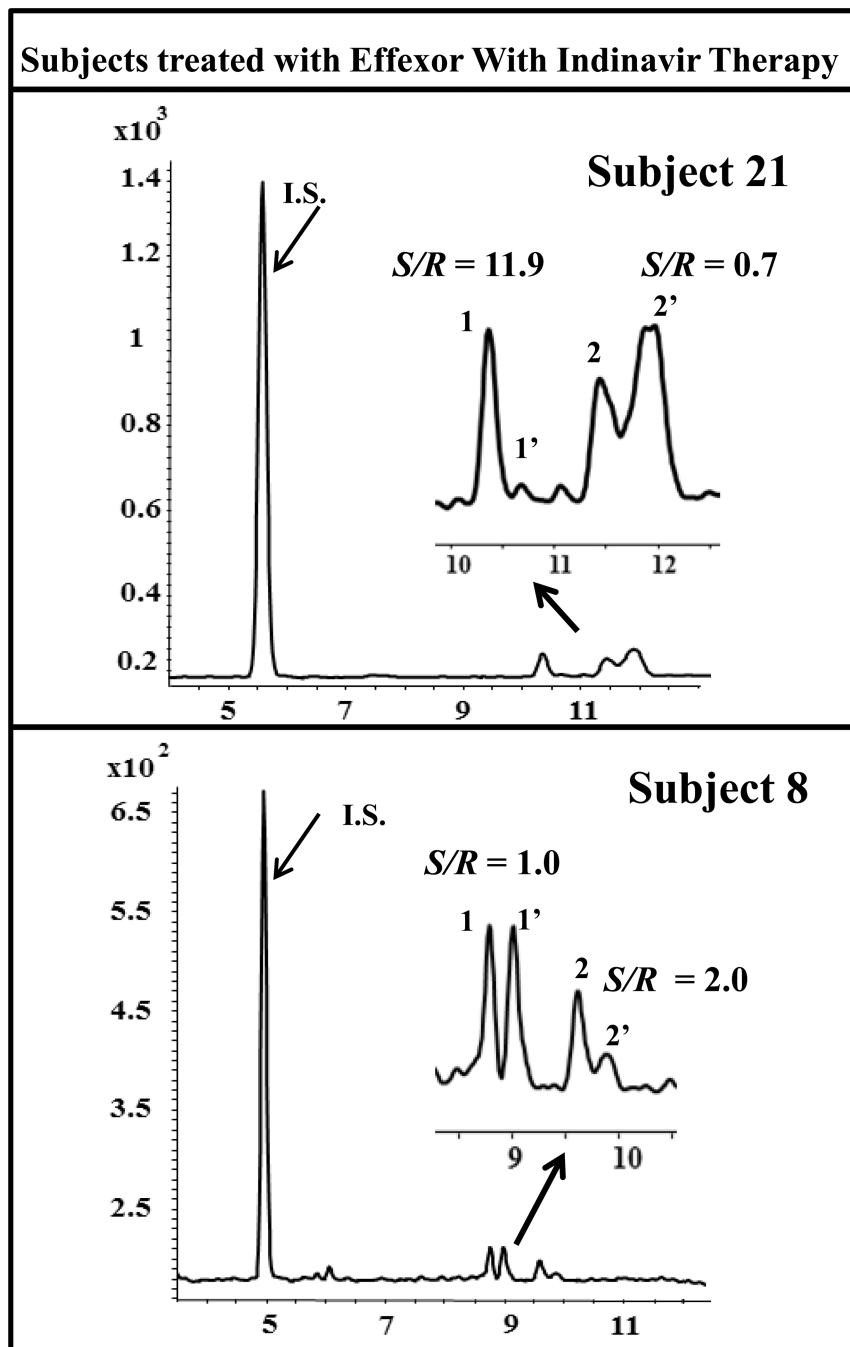


**Fig. 8.** Total ion electrochromatograms of subjects treated with VX without and with indinavir therapy at 1 hr and 4 hrs, respectively. The MEKC-MS/MS conditions are the same as in Fig. 2 except that 15 mM poly-L,L-SULA and 25 kV was used. (1,1' = *O*-DVX and 2,2' = VX). For subject 21:  $S/N_1 = 417$ ,  $S/N_{1'} = 32$ ,  $S/N_2 = 40$ ,  $S/N_{2'} = 60$ . For subject 8:  $S/N_1 = 447$ ,  $S/N_{1'} = 448$ ,  $S/N_2 = 7.2$ ,  $S/N_{2'} = 3.6$  for *S*- and *R*- enantiomer of *O*-DVX and VX, respectively

**Table 1**

<sup>1</sup>Recovery study at three different concentrations using solid phase extraction (SPE) method

Compound	low Concentration 150 ng/mL	medium Concentration 1350 ng/mL	high Concentration 5,000 ng/mL
<i>S-O-DVX</i>	105.1% ± 2.6%	106.1% ± 5.2%	109.7% ± 4.2%
<i>R-O-DVX</i>	99.7% ± 9.1%	101.8% ± 9.9%	98.6% ± 2.6%
<i>S-VX</i>	92.8% ± 4.6%	83.5% ± 9.8%	112.8% ± 7.5%
<i>R-VX</i>	82% ± 6%	99.5% ± 9.8%	95.1% ± 7.2%

<sup>1</sup>The recovery at each level was determined by comparing the ratio of the peak area of each enantiomer in the blank plasma sample to those of the peak area in pure standard solution

Author Manuscript

Author Manuscript

Author Manuscript

Author Manuscript



Method validation parameters for the determination of *O*-DVX, VX and Internal standard (IS, atenolol) in human plasma

**Table 2**

Validation parameters	relative peak area <sup>d)</sup>		relative migration time				peak area <sup>e)</sup>	migration time			
	O-DVX		VX		VX						
	S	R	S	R	S	R	S	R			
Interday repeatability (%RSD) (n=3) medium	4.1	9.2	8.8	2.4	2.5	2.6	3.1	3.0	13.0	2.0	2.0
	2.2	3.0	2.2	5.3	3.7	3.6	3.8	4.6	3.7	3.2	3.2
Intraday repeatability (%RSD) (n=3)	5.0	4.8	6.2	5.1	1.4	2.0	1.9	1.2	5.6	1.2	1.2
	7.7	6.5	5.2	7.9	1.3	2.1	2.0	1.3	7.0	1.3	1.3
limit of detection (ng/mL) <sup>b)</sup>	15	15	10.5	10.5							
limit of quantitation (ng/mL) <sup>c)</sup>	45	45	31	31							
	150–5000	150–5000	150–5000	150–5000							

<sup>a)</sup> Low, medium and high concentrations were 150, 1350 and 5,000 ng/mL for *S*- or *R*-ODVX and VX, respectively.

<sup>b)</sup> The limit of detection (LOD) was estimated at a signal-to-noise (*S/N*) ratio of 3.3

<sup>c)</sup> The limit of quantitation (LOQ) was estimated at *S/N* ratio of 10

<sup>d)</sup> The relative peak areas and relative migration times were calculated by taking the ratio of the peak area and migration time of each respective enantiomer to the I.S.

<sup>e)</sup> The peak areas and migration times of I.S. were calculated by taking the average of peak area and migration time of I.S.